Comparison of actuator disc and Joukowsky rotor flows, to explore the need for a tip correction

2015 J. Phys.: Conf. Ser. 625 012013

(http://iopscience.iop.org/1742-6596/625/1/012013)

Comparison of actuator disc and Joukowsky rotor flows, to explore the need for a tip correction

Gijs van Kuik[1], Wei Yu[1], Sasan Sarmast[2] and Stefan Ivanell[2]

[1]DUWIND, Faculty of Aerospace Engineering, TU-Delft, Kluyverweg 1, 2629HS Delft, the Netherlands

[2]Wind Energy Campus Gotland, Dept. of Earth Sciences, Uppsala University, 621 67 Visby, Sweden

E-mail: g.a.m.vankuik@tudelft.nl

Abstract. In van Kuik & Lignarolo (2015, *Wind Energy* accepted with modifications) potential flow solutions have been obtained for classical actuator discs (axisymmetric, uniform load) presenting a model for the non-uniformity of the axial velocity at the disc. Current rotor design models proceed from a disc with a uniform axial velocity, modified by a tip correction like the one of Prandtl-Glauert-Shen. A comparison shows that this correction leads to a similar distribution as obtained from the potential flow solutions. A next comparison is made with the velocity distribution at the blade position of a Joukowsky rotor with constant bound circulation, calculated by an Actuator Line and a Lifting Line model. The resulting distributions correspond reasonably well to the potential flow disc distribution, in magnitude as well as shape. This implies that this non-uniform distribution is relevant for a rotor with a finite number of blades, and could be the basis for rotor design instead of the uniform but tip-corrected distribution.

1. Introduction

Most Blade Element Momentum codes (BEM) proceed from the assumption that the optimal induction at the rotor plane is uniform, with a correction for the difference between a disc and a rotor. Most used is the Prandtl-Glauert tip correction F which is analysed and expanded by Shen *et al.* [1, 2]. Also aerodynamic optimizations using CFD (computational fluid dynamics) like Johansen *et al.* [3] assume that a uniform induction is best. However, as BEM codes apply actuator disc momentum theory, the assumption of uniform induction should find its basis in actuator disc flow solutions. In van Kuik & Lignarolo [4] the potential flow solutions for actuator discs with a uniform normal load have been presented. It is shown that not the axial component v_z is uniform but the absolute velocity $|\boldsymbol{v}|$. The non-uniform distribution for v_z denoted as G is a function of the local radius r and the thrust T. It shows slightly higher values than the disc-averaged value $\overline{v_{z,disc}}$ for relative radius $r/R < 0.8$ and lower values near the disc edge. This 'edge effect' is qualitatively the same as the 'tip effect' of F. This raises two questions:

(i) is it better to optimize a rotor based on the non-uniform distribution G instead of a uniform induction and correcting it by F?

(ii) how representative is the actuator disc velocity distribution for a rotor?

The rotor to be studied has B blades carrying a constant blade-bound circulation. Such a rotor was first analysed by Joukowsky [5] by which it is called a 'Joukowsky rotor'. This

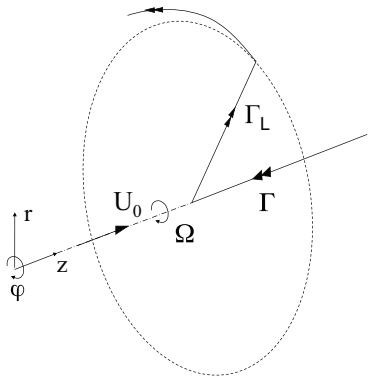

Figure 1. The coordinate system and orientation of the vortices, shown for one lifting line L

rotor becomes the disc with a uniform load after the limits $B \to \infty$ and tip speed ratio $\lambda \to \infty$ meanwhile keeping the converted power constant, see van Kuik [6]. The tip speed ratio is the tip speed ΩR divided by the wind speed U_0. The blades are modelled as lifting lines with prescribed constant bound circulation Γ_L, see figure 1, also showing the coordinate system (z, r, φ)[1]. The bound vortex continues as a root vortex at the axis and as a tip vortex at the wake boundary. All vortices have a kernel radius δ. The root vortex becomes $\Gamma = -B\Gamma_L$ or, dimensionless:

$$q = \frac{B\Gamma_L}{2\pi R U_0} \tag{1}$$

Note that the sign of Γ and q is different in order to obtain positive thrust and power coefficients.

First some general expressions for the thrust and power coefficients of a Joukowsky rotor are derived. Then the first question is discussed in section 3, by evaluating F for the three load cases in table 1, all for $B = 3$, and G for the disc with the same thrust coefficient. For the second question, two numerical models are used: a potential flow lifting line (LL) model and a computational fluid dynamic model using actuator lines (AL), both of which are briefly described in the appendix. Section 4 compares the results of both models with emphasis on the velocities at the rotor plane, where after section 5 compares all methods.

Table 1. Flow cases

Case #	λ	2λq
1	7	0.888
2	7	0.970
3	20	0.888

2. Expressions for the thrust and power of a Joukowsky rotor

Since the bound vorticity Γ_L of the lifting lines (L) is constant, simple expressions for the thrust and power are possible. The thrust and torque originate from the axial and azimuthal component of the Kutta-Joukowsky load L at Γ_L. The product of torque and Ω gives the power:

$$C_p = \frac{1}{\frac{1}{2}\rho U^3 \pi R^2} \rho \Omega B \Gamma_L \int_0^R v_{\boldsymbol{z},L} r dr = 2\lambda q \frac{\overline{v_{\boldsymbol{z},L}}}{U_0} \tag{2}$$

[1] In [4] the axis has the x-coordinate; the system is identical otherwise.

with $\frac{\overline{v_{z,L}}}{U_0} = \int_0^1 \frac{v_{z,L}}{U_0} d\left(\frac{r}{R}\right)^2$. The thrust is determined by the total axial load at the B lifting lines, $L_z = \rho B \Gamma_L (\Omega r - v_{\varphi,L})$. The expression for the thrust coefficient is:

$$C_T = \frac{\rho B \Gamma_L \int_0^R (\Omega r - v_{\varphi,L}) dr}{\frac{1}{2}\rho U^2 \pi R^2} = 2\lambda q - 4q \int_0^1 \frac{v_{\varphi,L}}{U} d\frac{r}{R} \tag{3}$$

The local thrust coefficient C_t defined as $dL_z / \left(\rho U_0^2 \pi r dr\right)$ becomes:

$$C_t = \frac{\rho B \Gamma_L (\Omega r - v_{\varphi,L})}{\rho U^2 \pi r} = 2\lambda q - 2q \frac{v_{\varphi,L}}{U} \frac{R}{r} \tag{4}$$

In the wake the azimuthally averaged value $\overline{v_\varphi} = \Gamma / (2\pi r)$ but in the rotor plane it is half this value: $\overline{v_{\varphi,x-0}} = \Gamma / (4\pi r)$. The azimuthal distribution of v_φ will be uniform for low values of r/R as the induction by the root vortex dominates. However, for larger r/R values the tip vortices will add a harmonic distribution. When the non-uniformity of v_φ is neglected, $v_{\varphi,L}/U \approx \Gamma / (4\pi r U)$ for $r > \delta$ and $\Gamma r / \left(4\pi\delta^2\right)$ for $r < \delta$. As the contribution of the area $\pi\delta^2$ to thrust and power is negligible, this contribution is omitted. The result is:

$$\left.\begin{aligned} C_T &= C_{T,\Delta P} + C_{T,\Delta\varphi} \\ C_{T,\Delta P} &= 2\lambda q \\ C_{T,\Delta\varphi} &= -4q \int_{\delta/R}^1 \frac{v_{\varphi,L}}{U} d\frac{r}{R} \approx -2q^2 \ln \frac{\delta}{R} \end{aligned}\right\} \tag{5}$$

and

$$\left.\begin{aligned} C_t &= C_{t,\Delta P} + C_{t,\Delta\varphi} \\ C_{t,\Delta P} &= 2\lambda q \\ C_{t,\Delta\varphi} &= -2q \frac{v_{\varphi,L}}{U} \frac{R}{r} \approx q^2 \left(\frac{R}{r}\right)^2 \end{aligned}\right\} \tag{6}$$

The first term at the right hand side of C_T and C_t is denoted $C_{T,\Delta P} = 2\lambda q$ since only this part of the thrust contributes to the conversion of power, see (2). The second term represents the contribution to the thrust by the radial pressure gradient balancing the radial distribution of v_φ. The singular logarithmic appears in C_p but not in C_T. However, it may have an indirect impact at C_p by $v_{z,L}$. With $\delta \ll R$ the singular term is positive, so it adds up to the thrust. For the hypothetical case of a potential flow model with a singular vortex when $\delta \to 0$, $C_{T,\Delta\varphi}$ becomes infinite. With the data of flow case 1: $2\lambda q = 0.8889$, $\lambda = 7$ and $\delta/R = 0.03$ which are values used in current rotor designs, $C_{T,\Delta\varphi} \approx 0.028$ so the thrust coefficient is somewhat higher than estimated in absence of $v_{\varphi,L}$. Apart from $C_{t,\Delta\varphi}$ the local thrust coefficient is constant.

The numerical results presented in the next section enable evaluation of the approximation $v_{\varphi,L} \approx q\frac{R}{2r}$ used in the expressions for $C_{T,\Delta\varphi}$ and $C_{t,\Delta\varphi}$. This appears to give a deviation $\Delta C_T = 0.0002$, and $\Delta C_t = 0.007$ close to the tip where $v_{\varphi,L}$ reaches a local minimum, see figure 5. The conclusion is that the approximation is well in place.

With (2), (5) and (6) the thrust and power coefficients are expressed in the independent parameters λ and q, and in the only unknown parameter $\overline{v_{z,L}}$. It is interesting to observe that (2) and (5) are identical to eq. 57 of Sørensen & van Kuik [7] except for the missing term $q^2/2$ accounting for the contribution of the vortex kernel. For the example values used here, this term contributes to C_T only 0.002 so is negligible indeed.

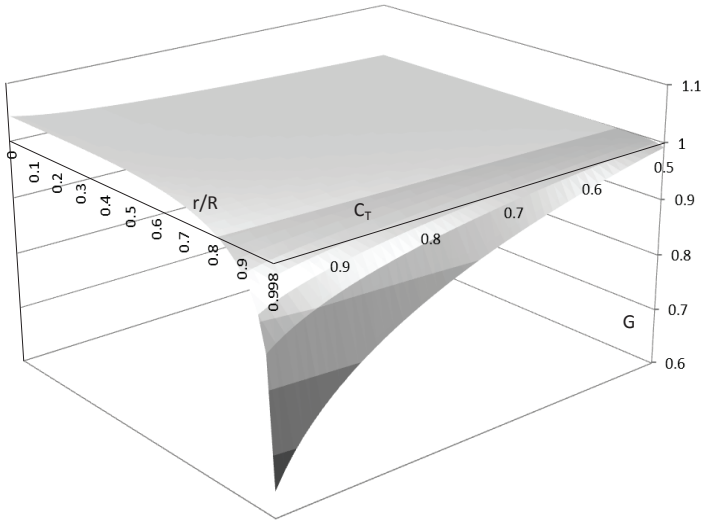

Figure 2. The velocity distribution function G (10) at the uniformly loaded actuator disc. As $\int_0^1 Gd(r/R)^2 = 1$ the plane $G = 1$ corresponds to $\overline{v_{z,disc}}$ as obtained by momentum theory.

3. Momentum theory with two non-uniform v_z distribution functions

In BEM models without any tip correction, the distribution of the axial velocity is determined by applying the local momentum equation $C_t = 4v_{z,L}(1-v_{z,L})$, where the local thrust coefficient $C_t = L_z/\left(\rho U_0^2 \pi r\right)$. Branlard *et al.* [8] and Shen *et al.* [1] have evaluated existing tip corrections with emphasis on the Prandtl-Glauert correction F given by eq. (2) of [1]. Shen *et al.* [2] have adapted this correction resulting in the Prandtl-Glauert-Shen (PGS) method with an additional correction F_1 to account for local tip shape properties:

$$\left.\begin{aligned} F_1 &= \frac{2}{\pi}\cos^{-1}\left[\exp\left(-g\frac{B}{2}\left(\frac{R}{r}-1\right)^n \frac{1}{\sin(\theta)}\right)\right] \\ g &= \exp\left[\frac{0.125\,(B\lambda-21)}{1-2k}\right]+0.1 \\ n &= 1+0.5k \end{aligned}\right\} \tag{7}$$

where θ is the local inflow angle with $\sin(\theta) = v_{z,L}/\sqrt{(\Omega r - v_{\varphi,L})^2 + v_{z,L}^2}$. For $n = 1$ and $g = 1$ F_1 is identical to F. k is the minimum value of chord-to-radius derivative at the tip, with $k = -0.45$ used in Shen's tuning. The same value is used here. With B, λ and q given in table 1 F and F_1 are known except for the induction $a_L = (1 - v_{z,L}/U_0)$. As in BEM the second relation between the induction and F, F_1 is the local momentum equation, to be solved for a_L :

$$C_t F_1 = 4a_L F(1 - a_L F), \tag{8}$$

with C_t now given by (6) instead of blade element theory. The q^2 term in (6) is neglected.

Van Kuik & Lignarolo [4] have derived a function G representing the radial distribution of v_z of actuator discs with an axisymmetric uniform load, based on a potential flow model for the wake. Classical momentum theory gives the average value of $\overline{v_{z,disc}}$ but not the distribution. Figure 2 shows that the local axial velocity decreases towards the disc edge, instead of being constant as often assumed in momentum balances. The distribution is given by:

$$v_{z,disc}(r, C_T) = G(r, C_T)\overline{v_{z,disc}(C_T)} \tag{9}$$

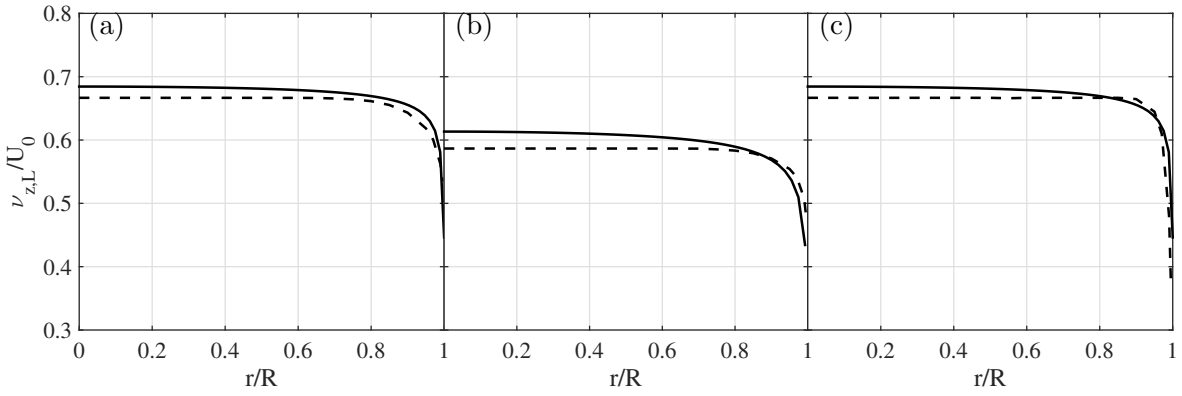

Figure 3. The axial velocity distribution obtained from the momentum theory + Prandtl-Glauert-Shen correction (dash line) and actuator disc function G (solid line). (a) Case 1, (b) Case 2 and (c) Case 3

with $\int_0^1 G d(r/R)^2 = 1$ so the disc-averaged momentum theory result remains the same. G is approximated by the surface-fit to the numerical results of [4]:

$$\left.\begin{array}{rcll} G(r,C_T) & = & 1+\alpha_1\left(1-1.00076\left(1-\left(\frac{r}{R}\right)^{\alpha_2}\right)^{0.0015}\right) & \\ \text{with} \quad \alpha_1 & = & 62.05(1-C_T)^{0.42}-47.56 & \\ \alpha_2 & = & 7-2.5C_T & \end{array}\right\} C_T \geq 0.5 \qquad (10)$$

$$\left.\begin{array}{rcll} G(r,C_T) & = & 1 & \end{array}\right\} C_T < 0.5 \qquad (11)$$

The local momentum equation to be solved is:

$$\left.\begin{array}{rcl} C_t & = & 4a(1-a) \\ 1-a_L & = & G(1-a) \end{array}\right\} \qquad (12)$$

C_t is given by (6) with the q^2 term omitted as before in solving (8). The first equation gives the induction a as if the local and disc-averaged momentum equations are the same, the second equation gives the local value. Unlike the PGS correction model the axial velocity is higher than predicted by the unmodified momentum equation for $r/R < 0.8$. This is shown in figure 3 presenting $v_{z,L}$ as resulting from the PGS correction and G function for the 3 load cases considered. For $r/R > 0.8$ the actuator disc line G corresponds reasonably well with the PGS tip correction model.

4. Comparison of the Actuator Line and Lifting Line results

Before the relevance of $G(r, C_T)$ for a rotor with a finite number of blades is investigated, the Actuator Line and Lifting Line codes used for this purpose will be compared and validated. Figure 4 shows the wake development as calculated by both methods for cases 1 and 2. The wake contour and the downstream positions of the tip vortices agree reasonably well.

Figure 5 compares the velocity components at the actuator or lifting line. For all three cases the azimuthal and radial components are identical except near the tip vortex where the differences in de-singularization become visible. Also the axial velocity distributions in case 3 match very well, while these differ slightly in case 1 and 2. This is caused by the discretization of

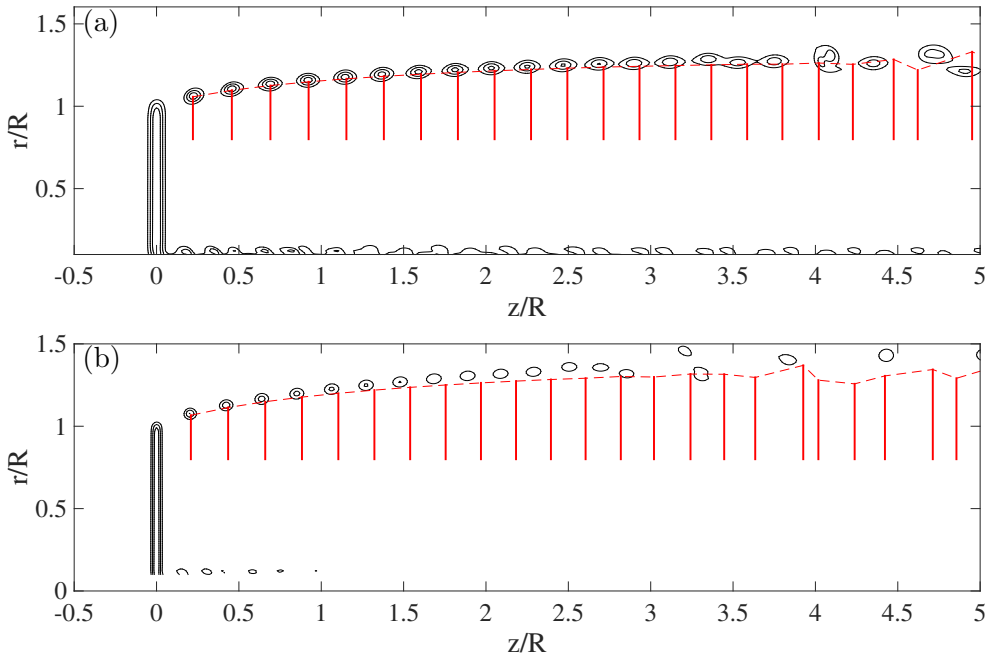

Figure 4. Azimuthal plane cut at the blade position $\phi = 0°$ for (a) case 1, (b) case 2. Case 3 is not shown as the AL-calculated vortices are not graphically discernible any more. Contours indicate the vorticity magnitude calculated from the AL approach. The dashed and solid red lines indicate the wake envelope and position of the vortex cores estimated from the LL approach.

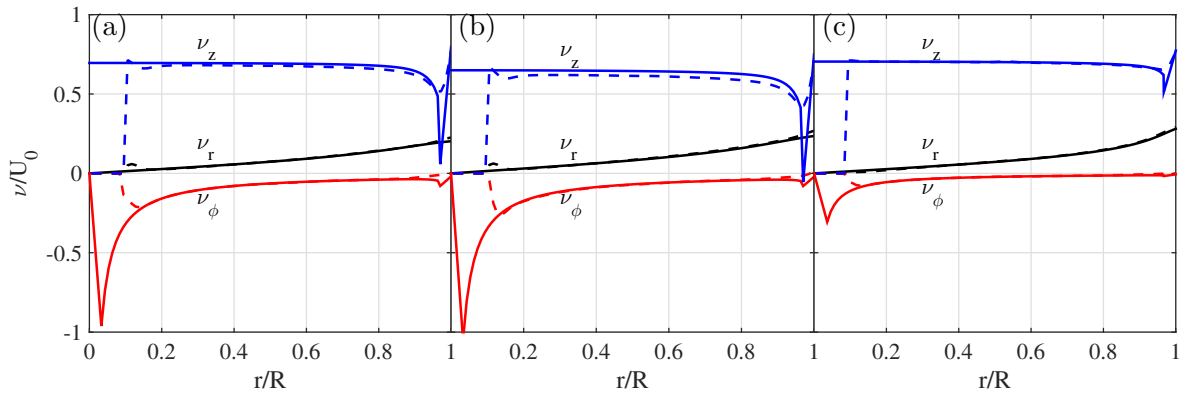

Figure 5. The velocity components at the actuator line (dash line) and lifting line (solid line) for (a) case 1, (b) case 2 and (c) case 3.

the tip vortices in the LL method, which is finer for increasing λ, as discussed in the appendix. As the correspondence of the results from both codes is quite good, no LL calculations with a finer discretization have been done.

Figure 6 shows the distribution of the axial velocity at the rotor plane. Again these distributions agree reasonably well except for $r < 0.1R$ and near the tip, due to differences in the desingularization of the vortices. The LL method assumes a Rankine vortex kernel with diameter δ, whereas in the AL approach the vortex structures are formed from a vortex sheet as a result of lift force distribution along the actuator line and the velocity fields are used to evaluate the vortex properties such as the vortex core size. With the LL method the sensitivity of the

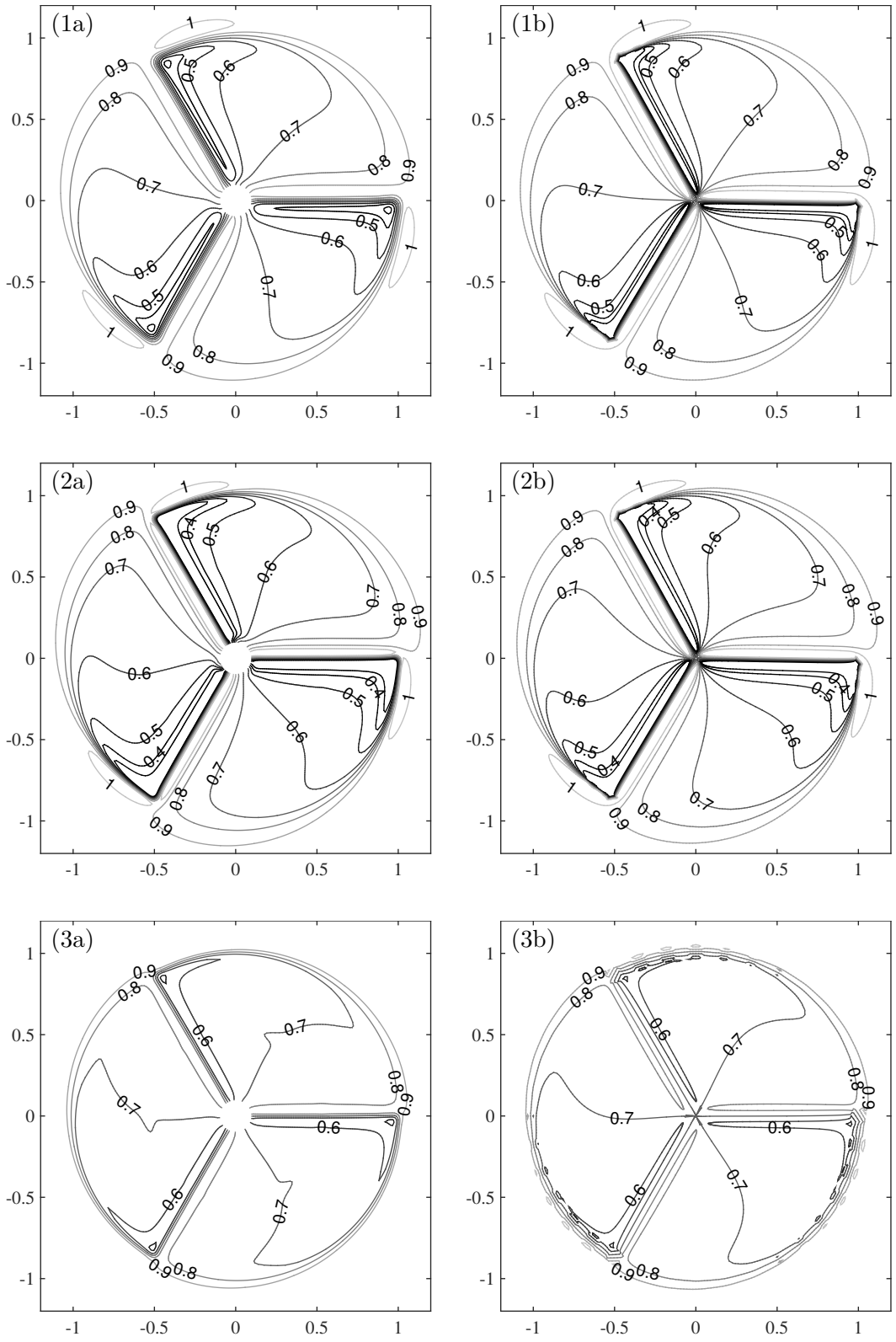

Figure 6. Distribution of v_z/U_0 at the rotor plane z=0 according to the actuator line (a), and lifting line (b) model, for flow case 1 (top), 2 (middle) and 3 (bottom).

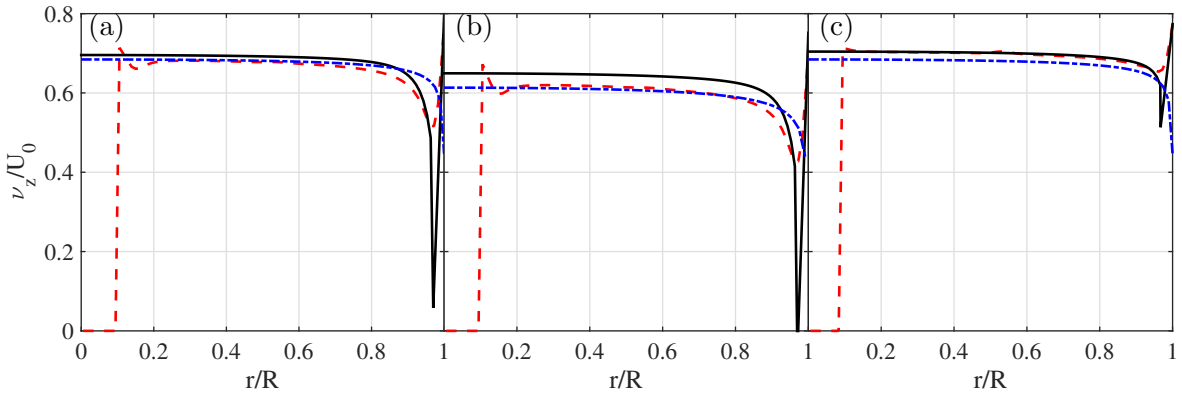

Figure 7. The axial velocity distribution at the actuator line (red dashed line), lifting line (black solid line) and actuator disc (blue dashed-dot line) for cases, (a) case 1, (b) case 2 and (c) case 3.

results for different δ has been tested. The distribution itself is invariant except for the area covered by the vortex kernel, as might be expected. The conclusion is that the de-singularization near the centre has no impact on the level and shape of the distributions. Figure 6, top row, corresponds well with figure 4(b) of Segalini *et al.* [9], showing the axial velocity for the same load case but with a different lifting line model.

5. Comparison of disc and rotor results

In figure 7 the distribution of the axial velocity of the actuator disc is compared with the distribution calculated by the AL and LL models at the blade position. For the inboard part, $r < 0.6R$, the disc distribution equals the AL distribution in cases 1 and 2, but is a bit lower than the AL and LL distributions in case 3. For this high λ case, the disc and AL-LL distributions match very well near the tip. For the lower λ cases 1 and 2, the AL and LL distributions correspond to the disc distribution at a slightly lower radius. This is to be expected since for a high λ the tip vortices are less strong compared to the low λ flow with equal thrust. The power and thrust coefficients according to the several methods are shown in table 2. The LL C_p values are consistently higher than the AL values, in accordance with the differences in axial induction.

Table 2. C_p and C_T as determined by eq.(2) respectively (5) with $\overline{v_{z,L}}$ from the AL and LL method, momentum theory plus PGS and G distributions, and the AL and LL simulation results, in % deviation from the actuator disc momentum theory values.

C_p	(2)+AL	(2)+LL	MT+PGS	MT+G	AL	LL
Case 1	-2.1	-2.0	-2.9	-0.3	-4.1	-2.0
Case 2	-0.4	2.2	-2.5	-1.4	-5.2	2.2
Case 3	4.0	3.2	-1.8	-0.3	1.3	3.4
C_T	(5)	(5)	MT	MT	AL	LL
Case 1	2.3	3.2	0.0	0.0	1.9	3.6
Case 2	3.0	3.5	0.0	0.0	2.1	3.9
Case 3	2.7	2.7	0.0	0.0	-0.1	0.4

The same holds for the momentum theory results obtained with the PGS or G function. The latter values are consistently higher since the average induction using the PGS function is higher compared to the G function values. With respect to C_T the analytical and AL-LL values are higher than the momentum theory values. The reason for this is the $C_{T,\Delta\varphi}$ term in (5). In particular case 2 shows $C_T > 1$ for the LL model. The AL and LL C_p values for case 3 are higher than the Betz-Joukowsky limit. Some of these observations are in line with the results obtained by Segalini *et al.* [9]. Figure 8 of this paper shows Lifting Line results for case 1 with $\delta = 0.03$, with C_T 3% higher than momentum theory gives, and C_p 4% lower. The results for C_p and C_T merit further investigation. However, this has no impact on the analysis of the present paper as this focuses on the non-uniformity of the velocities in the rotor plane as illustrated by the AL and LL results.

6. Evaluation and conclusions

The 2 research questions mentioned in the introduction lead to the following answers:

(i) The non-uniform induction at the actuator disc is accurately captured by the combination of momentum theory based on a uniform induction plus the correction by the Prandtl-Glauert-Shen model. In other words: when the non-uniform disc distribution is used as basis for BEM rotor design, the tip correction models do not need to correct for a higher induction - lower axial velocity near the tip. For the inboard region always $v_{z,disc} > v_{z,PGS}$.

(ii) The non-uniform distribution of $v_{z,disc}$ is reasonably well reproduced by the v_z distribution at the position of the bound vortex of a Joukowsky rotor, with the following remarks to be taken into account: the Actuator Line model and Lifting Line model show a very minor difference for the design thrust coefficient $C_T = 8/9$, $\lambda = 7$ and no difference for the same C_T, $\lambda = 20$ except at the tip itself. For $C_T = 0.97$, $\lambda = 7$ the difference in v_z is 5%. The shape of the disc distribution corresponds to the AL-LL distribution for $\lambda = 20$ while it corresponds to the AL-LL distribution for $\lambda = 7$ with a corrected, lower, radius.

A third conclusion is that the axial velocity field at the rotor disc calculated by the CFD and Potential Flow models are very similar, which confirms that the non-uniform distribution of the velocity does not depend on the type of model, but is an inherent feature of the flow.

The results for the Joukowsky rotor have shown that the non-uniform $v_{z,disc}$ distribution and the v_z distribution at the position of the blade of a rotor are similar, by which it is worth to consider the non-uniform $v_{z,disc}$ as basis for BEM, instead of a uniform $v_{z,disc}$ which needs a tip correction.

The physical or fluid dynamic origins of the Prandt-Glauert-Shen tip correction and the non-uniform velocity distribution G are different, so the good correspondence is remarkable. The tip correction as formulated by Prandtl is a correction of actuator disc results for the finite number of blades, by considering the non-uniform velocity field of the wake represented by helical vortex sheets. The effect of it is most noticeable near the edge of the streamtube, by which it has been named tip correction. Thereafter Prandtl's model has been adapted and calibrated by Glauert and Shen so it has become a calibrated engineering model for the flow non-uniformity. The good correspondence with the flow non-uniformity as calculated by actuator disc potential flow field solutions and with the Actuator-Lifting Line calculations may be considered as a confirmation of this calibration.

Acknowledgments

The Lifting Line simulations of TU-Delft were performed with financial support from the China Scholarship Council. The Actuator Line simulations of Uppsala University, campus Gotland, were performed on resources provided by the Swedish National Infrastructure for Computing (SNIC) within the project SNIC 2014/8-5.

Appendix

The Lifting Line model

The model is structured as shown in figure 1: the blades are modelled as bound vortices with constant strength Γ_L rotating with angular velocity Ω, the root vortex $\Gamma = B\Gamma_L$ is located at $r = 0$, the tip vortices with strength Γ_L are released at $r = R$ and are discretized by piecewise straight vortex elements. Using the Biot-Savart law for the induction by each element, the total induction at each point in space is calculated. The convection of the tip vortices is driven by the velocity acting at the elements, being the sum of the total induction and the free stream velocity. The kernel of all vortices is a Rankine vortex with radius δ.

At time $t = 0$ the first element of the B tip vortices is released, with new elements following after each time step $\Delta t = \Delta\varphi/\Omega$. The calculation proceeds until the wake has developed so far that the induced velocities at the rotor-plane do not change any more. This is checked by the convergence of C_T and C_p. The values for δ and $\Delta\varphi$ are given in table 3.

The Actuator Line model

The computational fluid dynamic computations are carried out using a three-dimensional flow solver developed by Sørensen and Michelsen [10, 11] called EllipSys3D. It solves the discritized incompressible Navier–Stokes equations using a finite volume approach. In computations, the flow around the rotor is simulated using the actuator line approach [12]. In this approach, the presence of the actual rotor is approximated by the body forces which are distributed radially among the computational grid points in a 3D Gaussian manner. In order to impose the constant circulation $\Gamma = L/\rho v_{rel}$ (L indicates the lift while v_{rel} is the relative velocity), the distribution of L along the actuator line is evaluated manually. The drag is considered to be zero.

The computations are performed using an axisymmetric polar grid with approximately 49 million grid points. In the vicinity of the actuator lines around 35 million grid points are used in order to resolve the near-wake dynamics. Each blade is represented by 91 grid points along the actuator lines. The simulations are conducted in a rotating reference frame.

Table 3. Numerical parameters in the computations. Lifting line: column 2 & 3 , Actuator Line 4 & 5

Case #	$\Delta\varphi$ (^{o})	δ/R	$\epsilon/\Delta r$	δ/R
1	5	0.03	4	0.08
2	5	0.03	2.5	0.05
3	10	0.05	2.5	0.05

References

[1] WZ Shen, R Mikkelsen, JN Sørensen, and C Bak. Tip loss corrections for wind turbine computations. *Wind Energy*, 8(4):457–475, 2005.
[2] WZ Shen, WJ Zhu, and JN Sørensen. Study of tip loss corrections using CFD rotor computations. *J. Phys. Conf. Ser.*, 555:012094, 2014.
[3] J Johansen, M Gaunaa, and C Bak. Design of a Wind Turbine Rotor for Maximum Aerodynamic Efficiency. *Wind Energy*, 12:261–273, 2009.
[4] GAM. van Kuik and LEM Lignarolo. Potential flow solutions for energy extracting actuator disc flows. *Wind Energy*, accepted pending a minor revision, 2015.
[5] NE Joukowsky. *Theory Tourbillionnaire de l'Helice Propulsive, Article I.* Gauthier-Villars, Paris, 1912.
[6] GAM van Kuik. The relationship between loads and power of a rotor and an actuator disc. *J. Phys. Conf. Ser.*, 555:012101, 2014.
[7] JN Sørensen and GAM van Kuik. General momentum theory for wind turbines at low tip speed ratios. *Wind Energy*, 14:821–839, 2011.
[8] E Branlard, K Dixon, and M Gaunaa. Vortex methods to answer the need for improved understanding and modelling of tip-loss factors. *IET Renewable Power Generation*, 7(4):311–320, 2013.
[9] A Segalini and PH Alfredsson. A simplified vortex model of propeller and wind-turbine wakes. *J. Fluid Mech.*, 725:91–116, 2013.
[10] JA Michelsen. Block structured multigrid solution of 2D and 3D elliptic PDE's, AFM 94-06. Technical report, Dept. Fluid Mechanics, Technical University Denmark, Lyngby, 1994.
[11] NN Sørensen. General purpose flow solver applied to flow over hills. *PhD thesis, Risø*, 1995.
[12] JN Sørensen and WZ Shen. Num. Modeling of Wind Turbine Wakes. *J. Fluids Eng.*, 124(2):393–399, 2002.